Optics Letters

Supermode noise mitigation and repetition rate control in a harmonic mode-locked fiber laser implemented through the pulse train interaction with co-lased CW radiation

V. A. Ribenek,[1] D. A. Korobko,[1,*] A. A. Fotiadi,[2,3] and J. R. Taylor[4]

[1]Ulyanovsk State University, 42 Leo Tolstoy Street, Ulyanovsk, Russian Federation, 432017, Russia
[2]Electromagnetism and Telecommunication Department, University of Mons, Mons, B-7000, Belgium
[3]Optoelectronics and Measurement Techniques Unit, University of Oulu, Oulu, Finland
[4]Femtosecond Optics Group, Department of Physics, Imperial College London, London SW7, UK
*Corresponding author: korobkotam@rambler.ru

Received 9 August 2022; revised 14 September 2022; accepted 15 September 2022; posted 19 September 2022; published 30 September 2022

We report on new, to the best of our knowledge, techniques enabling both the mitigation of supermode laser noise and highly precise setting of the pulse repetition rate (PRR) in a soliton harmonically mode-locked (HML) fiber laser employing nonlinear polarization evolution (NPE). The principle of operation relies on resonant interaction between the soliton pulses and a narrowband continuous wave (CW) component cooperatively generated within the same laser cavity. In contrast to our recent findings [Opt. Lett. 46, 5747 (2021) and Opt. Lett. 46, 5687 (2021)], the new methods are implemented through the specific adjustment of the HML laser cavity only and do not require the use of an external tunable CW laser source.

https://doi.org/10.1364/OL.472780

Harmonically mode-locked (HML) fiber lasers delivering pulses with a pulse repetition rate (PRR) in the sub-GHz and GHz ranges have become a valuable alternative to semiconductor and solid-state lasers ensuring high beam quality, simplicity in adjustment, reliability, and user-friendly light output inherent to laser configurations in all-fiber format. The main drawback of HML laser technology is the noise-induced irregularities of the time interval between pulses known as the HML timing jitter. Generally, its value is much higher than that of mode-locked lasers operating at the fundamental frequency [1,2]. Therefore, physical mechanisms enabling jitter reduction in HML fiber lasers are of great practical importance [3–9]. The role of background radiation as a mediator providing the equalizing interaction between pulses has been extensively discussed in this context [10–12]. In addition, the idea of manipulating HML through continuous wave (CW) injection has been introduced and investigated [13], including the cases where the CW forces the laser to operate HML [10,11]. Recent studies of the transient processes in the HML laser have confirmed the importance of the pulse interaction with the background radiation in the buildup or annihilation of soliton pulses [14].

Ensuring low-level supermode noise and precise PRR tuneability in all-fiber-integrated HML laser sources establishes a new level of their versatility and extends areas of their application. Recently we reported on two new techniques [15,16] enabling control of a soliton HML fiber laser built on the principle of nonlinear polarization evolution (NPE). The methods exploit direct injection of narrowband CW from an external laser source into the HML laser cavity and rely on an appropriate adjustment of the CW laser wavelength relative to the HML laser soliton spectrum.

Practical implementation of these techniques requires the use of an external narrowband CW laser source supplementing the HML laser. A narrow linewidth (<0.1 nm), linear polarization state, and an output power of a few mW are key CW laser characteristics essential for the application. Tunability of the CW laser wavelength is also important, since it is used to select the position of the injected narrowband signal within the HML laser spectrum enabling its resonant interaction with the soliton pulse train and/or background radiation inside the HML laser cavity. The need to use an external CW laser source in combination with the HML laser clearly increases the cost of the system and limits the range of its possible applications.

In this Letter, we present a resonant CW injection concept offering new solutions for advanced HML laser control, avoiding the use of an external CW laser source. Instead, we exploit a simple adjustment to the HML laser, ensuring the cooperative generation of the soliton pulse train and a narrowband CW signal in the same laser cavity. Indeed, the CW lasing is known to sometimes accompany the HML laser operation [9,17]. With an optimized laser, a CW component generated simultaneously with the soliton pulse train can trigger the transition processes inside the HML laser cavity, resulting in the birth or annihilation of individual solitons in one considered scenario, and suppression of the supermode noise level in another. We explore the potential of these effects for supermode noise mitigation and

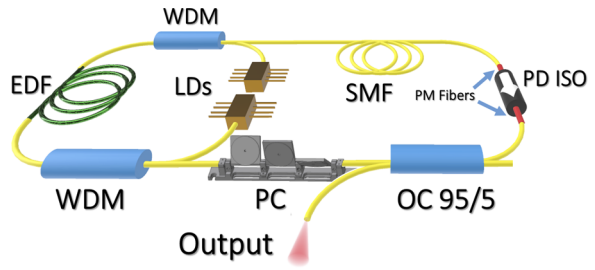

Fig. 1. Experimental HML laser setup.

precise PRR control in the HML laser, highlighting the advantages and drawbacks of the new techniques compared to the optical injection solution.

The experimental configuration of an Er-doped, soliton, NPE mode-locked fiber ring laser is shown in Fig. 1. The laser cavity consists of two types of fibers: a 0.8 m length of heavily erbium-doped fiber (EDF) with normal dispersion (–48 ps/nm/km) and a standard single-mode fiber (SMF-28) with anomalous dispersion (17 ps/nm/km). The 15.5 m total length of the laser cavity provides a fundamental PRR f_0 = 13.3 MHz. A polarization-dependent fiber isolator (PD ISO) supplied by output PM fibers (~0.5 m), two 980/1550 WDM couplers, a 3-paddle fiber polarization controller (PC), and a 5% output coupler (OC) constitutes the fiber birefringence filter incorporated into the cavity. The filter spectral transmittance maxima (FTM) are spaced with a period of ~16 nm and their positions are determined by the net cavity birefringence [18] that does not change over all the experiments. The cavity is placed in a foam box to reduce the influence of the lab environment. The laser is pumped at 980 nm from two laser diodes specified for a maximum power of 550 mW. The laser operation is monitored by an optical spectrum analyzer (Yokogawa 6370D) with a resolution of 0.02 nm and a radio frequency spectrum analyzer (R&S FSP40) coupled with a 30-GHz photodetector.

Commonly, the operational wavelength of the laser can be selected by a coarse PC adjustment from a few spectral bands between 1550 and 1590 nm specific to the built fiber configuration. Selection of the laser wavelength to the limited range 1563–1575 nm enables the specific regime of laser operation considered in this Letter. In this regime, the soliton pulse train and the CW component are generated concomitantly in the same laser cavity. Alteration of the laser pump power and adjustment of the PC are the only means used here to control laser operation in all the experiments. Figure 2 highlights the details of the laser

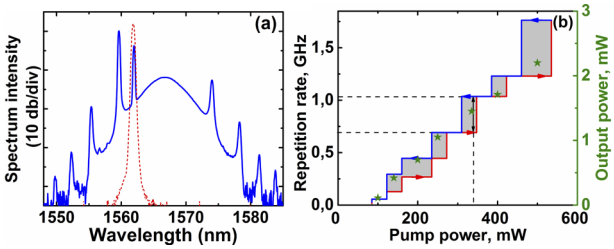

Fig. 2. (a) Laser optical spectra recorded at a pump power of ~40 mW (CW operation, red dotted line) and 450 mW (HML soliton trains, PRR~1.23 GHz, blue solid line). (b) PRR as a function of the increasing (red line) and decreasing (blue line) pump power. The PC settings are fixed. The gray areas show the PRR range subjected for the PRR precise setting. Green asterisks show the output power.

operation at $\lambda \sim 1567$ nm. The laser exhibits two distinct pump power thresholds associated with the start of the CW and then pulse train generation. The first threshold is achieved at a pump power of ~30 mW and results in a single narrow peak at 1562 nm observed in the optical spectrum analyzer [Fig. 2(a), dotted line]. Importantly, the absolute CW line position always coincides with one of FTMs and remains fixed during all the experiments. The second laser threshold is achieved at a pump power of ~80 mW, when the mode-locking regime is established. With the pump power in the range of ~80–120 mW, the laser emits regular pulses with a fundamental PRR f_0. In this regime, only one soliton circulates in the laser cavity. With a further increase of the pump power, the laser switches to multi-pulse operation. A fine adjustment of the PC at this stage equalizes the temporal distribution of the generated pulses inside the cavity, thus enabling HML. In the HML regime, the laser emits regular pulses with the PRR equal to N pulses per cavity round trip $f_{rep} = Nf_0$. The PRR could be controlled by an increase or decrease in pump power. We have checked that the pulses generated by the HML laser are close to the transform-limited solitons. The pulse width measured by the autocorrelator is ~0.5 ps (FWHM) and the spectrum width is ~5.5 nm (FWHM) giving the time-bandwidth product ~0.335 (at pump power ~200 mW).

Figure 2(b) shows the typical evolution of the laser PRR with the total pump power (both laser diodes contribute equally). As long as the PC settings are fixed, the presented data are completely reproducible. The total pump power is increased to 550 mW and then decreased to ~80 mW. At the maximal pump power of ~550 mW, the PRR is ~1.75 GHz. The red and blue lines highlight the soliton hysteresis effect [19], reflecting instantaneous PRR changes in the cases of increasing and decreasing pump power. The positive or negative PRR jumps $\Delta f_{rep} = \Delta m f_0$ are associated with simultaneous birth or annihilation of $|\Delta m|$ solitons. The peak soliton power could be estimated from the average laser power.

Above the second threshold, the laser exhibits operation typical of HML lasers based on the NPE mechanism. However, the CW lasing signature always overlaps the HML laser spectrum. The absolute position of the soliton spectrum (as a whole) relative to the CW component could be tuned smoothly over a range of ±5 nm using a precise PC adjustment [18]. This procedure commonly does not affect the HML laser operation nor the absolute position of the CW line. However, in some special cases, it could enable resonant interaction between the soliton train and the generated CW and, in that way, trigger the transition processes inside the HML laser cavity resulting in a change in the laser performance characteristics. Below we describe two effects, (1) supermode noise mitigation, and (2) birth and annihilation of the individual solitons, implemented into the HML laser operation via PC tuning.

The supermode noise mitigation effect is illustrated in Figs. 3 and 4. At a pump power of 450 mW, the HML laser operates with regular soliton pulses at a PRR of 1230 MHz monitored by the RF spectrum analyzer. The RF spectrum is typical of HML lasers. The main peaks of the RF spectrum are equally spaced by the PRR, whereas the surrounding small peaks are spaced by the fundamental PRR f_0 [Fig. 4(a)]. The ratio between the main peak amplitude and the maximum amplitude of the surrounding supermodes is referred to as the supermode noise suppression level (SSL) which is a key HML laser parameter characterizing the periodicity of pulse emission (the timing jitter). For the presented laser operation, the SSL value is ~24.5 dB.

The corresponding laser optical spectra are shown in Fig. 3. They exhibit Kelly sidebands associated with the intracavity generation of dispersive waves. A generated CW component is also presented in the HML laser spectrum and located between the spectrum maximum and the nearest Kelly sideband. To achieve the effect, using a fine adjustment of the PC, the soliton spectrum is shifted such that the Kelly sideband shifts toward the CW peak. Once a critical distance to the CW peak is reached (Fig. 3), the Kelly sideband (together with the HML spectrum as a whole) continues the movement without the requirement of further adjustment of the PC, reaching the CW line and absorbing it [Fig. 3(c)]. This behavior is accompanied by some spectral spikes [see Fig. 3(b)] and caused by the four-wave mixing between the CW light and dispersive waves (associated with the Kelly sideband) resulting in their final phase-matching [13]. Simultaneous to this process, the supermode noise level monitored by the RF analyzer is reduced by ~27 dB, i.e., the SSL increases to 51.5 dB [Fig. 4 (a), red line]. Direct timing jitter measurements also highlight a decrease from 7.7 to 2.1 ps.

A similar procedure was applied to the HML laser operating at different pump powers to reveal the PRR range available for the supermode noise mitigation effect. The results of this study are presented in Fig. 4(b). In all cases, as soon as the PC adjustment provides a certain initial shift of the Kelly sideband toward the CW line, the Kelly sideband continues to move that way until they merge (see Visualization 1). The last process is accompanied by a decrease in the supermode noise level at least by two orders of magnitude within a PRR range of 300 to 1230 MHz (see Visualization 2) and makes no other effect on the HML laser performance characteristics. The maximum SSL benefit of 32 dB is obtained for the laser operating with pulses at a PRR of 440 MHz. For a PRR >1230 MHz, the SSL reduction in the HML laser becomes less pronounced and is ~5 dB for 1720 MHz.

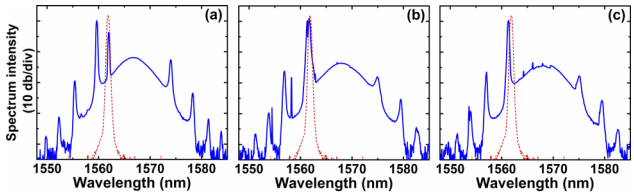

Fig. 3. Evolution of the optical HML laser spectrum during the supermode noise suppression process: (a) initial state, (b) Kelly sideband shifted toward the CW lasing line, (c) final state, the Kelly sideband absorbs the CW lasing line.

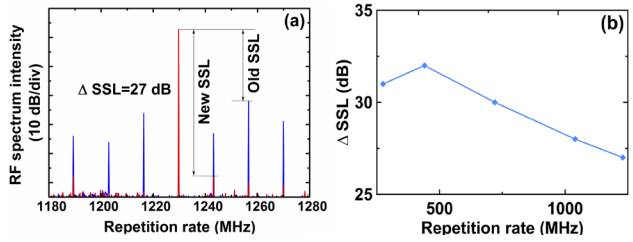

Fig. 4. (a) Modification of the HML laser RF spectrum caused by the supermode noise suppression process shown in Fig. 3 (initial state, blue line; final state, red line). (b) Changes of the SSL (Δ SSL) as a function of the HML laser PRR.

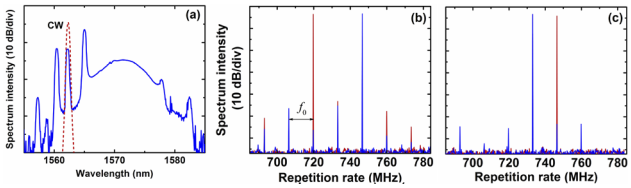

Fig. 5. The HML laser optical spectrum demonstrating the mutual position of the soliton spectrum (Kelly sideband) and CW lasing line enabling spontaneous PRR changes. (a) CW line recorded at the pump power of 40 mW (red dotted line) shown for comparison. (b) HML laser RF spectra (red line) before and (blue line) after the PRR switching by $+2f_0$ from 720 MHz up to 748 MHz, and (c) by $-f_0$ from 748 MHz down to 734 MHz. The RF spectrum resolution is 100 kHz. The spectra are recorded at a pump power of ~330 mW.

The second case of resonant interaction between the soliton pulse train and the generated CW component (Fig. 5) illustrates the birth and annihilation of individual solitons in the HML laser cavity. The effect is induced by appropriate manipulation of the PC and can be applied to control the PPR in the HML laser cavity which is unachievable through power variation alone. The blue and red curves shown in Fig. 2(b) highlight the rather limited number of PRR values achievable with the pump power control alone. An increase or decrease of pump power causes the PRR to jump by a large positive or negative value $\Delta f_{rep} = \Delta m f_0$, associated with the simultaneous generation or annihilation of a large number of solitons ($\Delta m >> 1$, typically 10–30). So, many intermediate PRRs (several hundreds of MHz) remain unachievable.

In contrast, manipulation of the soliton spectrum position relative to the position of the CW line using PC adjustment enables precise PRR setting to any discrete value within the gray areas marked in Fig. 2(b). One can obtain this result in a few steps. First, the pump power is set to be within the selected gray area. For example, for the precise PRR setting in the range ~720–1030 MHz [i.e., along the black arrow shown in Fig. 2(b)], the pump power is set at ~ 330 mW. Second, using fine PC adjustment, the soliton spectrum is smoothly shifted until it gets to the position where resonant interaction of the CW with the soliton pulse train takes place. We have observed that the resonance interaction occurs when the CW peak coincides within a relatively narrow area between two Kelly sidebands, as shown in Fig. 5(a). It manifests as instability in the HML laser spectrum observed around the CW line. This instability is also accompanied by a permanent change of the laser PRR passing all values within the gray area. The RF analyzer monitors this endless process in real-time. We have observed the main peak of the RF spectrum randomly walking within the 720–1030 MHz range. It is worth noting that setting of the pump power closer to the red line (within the gray area) accelerates the PRR changes in a positive direction, whereas setting of the pump power closer to the blue line accelerates the negative PRR changes. Finally, using a precise PC adjustment, once more, the PRR switching process could be interrupted at any moment by reverse shifting the soliton spectrum from its resonance position. After that, the PRR does not change, and the main peak of the RF spectrum maintains its last position. In this way, the PRR could be set to any desired value within the gray area, enabling laser operation at any harmonic of the ring cavity numbered 54 to 77. For example, Fig. 5(b) compares the initial and final RF spectra

associated with the PRR switching from 720 to 748 MHz by the step $2f_0$. Similarly, Fig. 5(c) illustrates the PRR changing from 748 to 734 MHz with the elementary step $-f_0$ implemented by the same method.

It is worth noting that the PRR switching procedure does not affect the HML laser SSL nor the pulse train stability. Similar experiments performed at different pump power levels confirm that the described PRR setting is achievable for any gray area marked in Fig. 2(b), thus extending the range available for precise PRR setting over the complete range up to 1750 MHz. In the discussed technique, the pump power level provides a coarse adjustment of the PRR, while the control of resonant interaction between the pulse train and co-lased CW component provides a precise PRR setting at the level of single soliton pulses (or FSR in the RF domain) via addition or subtraction. The typical evolution of the optical and RF laser spectra associated with the advanced PRR tuning are illustrated in accompanying Visualization 3 and Visualization 4.

The new experimental observations presented in this Letter should be considered in the context of our previous findings [13,15,16]. The implementation of similar phenomena in HML laser systems employing CW injection and CW lasing are comparable and rely on the same physical mechanisms.

The result of CW interaction with the HML laser radiation in the ring cavity depends on the position of the HML laser optical spectrum (Kelly sidebands) relative to FTM bands (1), the CW wavelength (2), power (3), and polarization state (4). The principal difference between the two approaches is the different number of system parameters that should be controlled simultaneously to implement the effects. In the laser system based on optical injection, all CW parameters are set independently using three PCs and external CW laser wavelength tuning. The laser employing the CW lasing is supplied with a single PC used for precise adjustment of the HML laser optical spectrum position (1) only.

The surprising phenomena considered in this Letter are caused by the resonant interaction between the CW and HML laser radiation. In this regime, the wavelength of the CW radiation circulating inside the HML laser cavity coincides with one of the FTM bands and the CW polarization state is the same as that of the HML laser. In the laser system based on optical CW injection, these conditions are provided by directly setting the CW polarization and wavelength. In the laser system based on the CW lasing, the CW lasing itself enables self-adjustment of the CW wavelength (2) and polarization state (4) enabling perfect resonance with the HML radiation. Importantly, the intracavity CW linewidth and power meet the requirements of the CW characteristics described in our previous work [15,16].

The resonant interaction between the CW and HML radiation can cause the birth or annihilation of individual solitons circulating inside the HML laser cavity. This process is stimulated by the modulation of the laser gain provided by the interference between the CW and pulsed radiation and can be governed by altering the CW power level. The laser system based on optical injection employs a direct CW power adjustment, whereas the laser based on CW lasing involves alteration of the HML spectrum position relative to the CW line. Both methods enable one-by-one PRR tuning.

Implementing the supermode noise suppression effect, one should enable resonant interaction between the intracavity CW and the dispersive wave produced by the HML soliton radiation. For this purpose, similarly in both lasers, the Kelly sideband (together with the HML laser spectrum) is shifted toward the position of the CW line using a PC adjustment. This triggers the transition dynamical processes evolving identically in both lasers and results in the supermode noise reduction.

In conclusion, we have explored an elegant and simple solution enabling dramatic improvement of the HML laser performance characteristics. The supermode noise is suppressed by two to three orders of magnitude and precise PRR setting is achieved in the extended tuneability range of 13–1750 MHz with a simple adjustment to the HML laser ensuring the cooperative generation of the soliton pulse train and a narrowband CW lasing component in the same laser cavity. Importantly, the triggered transition processes exhibit a resonant nature and do not affect other laser performance characteristics. One could translate new solutions to other laser configurations that rely on an external CW injection to avoid using an external CW laser source. We believe that our findings offer important insights into the HML laser dynamics associated with the interaction between background radiation and solitons that are crucial for HML laser design and optimization.

Funding. Russian Science Foundation (19-72-10037P); Ministry of Education and Science of the Russian Federation (075-15-2021-581); European Commission (101028712).

Disclosures. The authors declare no conflicts of interest.

Data availability. Data underlying the results presented in this paper are not publicly available at this time but may be obtained from the authors upon reasonable request.

REFERENCES

1. F. Rana, H. L. Lee, R. J. Ram, M. E. Grein, L. A. Jiang, E. P. Ippen, and H. A. Haus, J. Opt. Soc. Am. B **19**, 2609 (2002).
2. R. V. Gumenyuk, D. A. Korobko, and I. O. Zolotovskii, Opt. Lett. **45**, 184 (2020).
3. M. Nakazawa, K. Tamura, and E. Yoshida, Electron. Lett. **32**, 461 (1996).
4. O. Pottiez, O. Deparis, R. Kiyan, M. Haelterman, P. Emplit, P. Mégret, and M. Blondel, IEEE J. Quantum Electron. **38**, 252 (2002).
5. J. Schröder, D. Alasia, T. Sylvestre, and S. Coen, J. Opt. Soc. Am. B **25**, 1178 (2008).
6. L. Yuhua, L. Caiyun, W. Jian, W. Boyu, and G. Yizhi, IEEE Photonics Technol. Lett. **10**, 1250 (1998).
7. G.-R. Lin, M.-C. Wu, and Y.-C. Chang, Opt. Lett. **30**, 1834 (2005).
8. D. A. Korobko, D. A. Stoliarov, P. A. Itrin, V. A. Ribenek, M. A. Odnoblyudov, A. B. Petrov, and R. V. Gumenyuk, J. Lightwave Technol. **39**, 2980 (2021).
9. H. J. Kbashi, S. V. Sergeyev, M. Al-Araimi, A. Rozhin, D. Korobko, and A. Fotiadi, Opt. Lett. **44**, 5112 (2019).
10. G. Semaan, A. Komarov, M. Salhi, and F. Sanchez, Opt. Commun. **387**, 65 (2017).
11. A. Komarov, K. Komarov, A. Niang, and F. Sanchez, Phys. Rev. A **89**, 013833 (2014).
12. C. Lecaplain and P. Grelu, Opt. Express **21**, 10897 (2013).
13. D. A. Korobko, V. A. Ribenek, D. A. Stoliarov, P. Mégret, and A. A. Fotiadi, Opt. Express **30**, 17243 (2022).
14. J. Zeng and M.Y. Sander, Opt. Lett. **45**, 5 (2020).
15. V. A. Ribenek, D. A. Stoliarov, D. A. Korobko, and A. A. Fotiadi, Opt. Lett. **46**, 5747 (2021).
16. V. A. Ribenek, D. A. Stoliarov, D. A. Korobko, and A. A. Fotiadi, Opt. Lett. **46**, 5687 (2021).
17. Z. X. Zhang, L. Zhan, X. X. Yang, S. Y. Luo, and Y. X. Xia, Laser Phys. Lett. **4**, 592 (2007).
18. W. S. Man, H. Y. Tam, M. S. Demokan, P. K. A. Wai, and D. Y. Tang, J. Opt. Soc. Am. B **17**, 28 (2000).
19. D. Y. Tang, B. Zhao, L. M. Zhao, and H. Y. Tam, Phys. Rev. E **72**, 016616 (2005).